*HIPPOCAMPUS 14:232–243 (2004)*

# Properties of Horizontal Axo-axonic Cells in Stratum Oriens of the Hippocampal CA1 Area of Rats In Vitro

Paul Ganter,[1,2*] Peter Szücs,[1] Ole Paulsen,[1,2] and Peter Somogyi[1]

**ABSTRACT: Local-circuit γ-aminobutyric acid (GABA)ergic interneurons constitute a diverse population of cells, which remain poorly defined into functionally distinct subclasses. Traditionally, dendritic and axonal arbors have been used to describe cell classes. In the present report, we characterize a set of hippocampal interneurons, horizontal axo-axonic cells, located in stratum oriens. They displayed the pattern of axonal arborization characteristic of axo-axonic cells with radially aligned rows of boutons making synapses exclusively on axon initial segments of pyramidal cells, as shown by electron microscopy. However, in contrast to previously described axo-axonic cells, which have radial dendrites spanning all layers, the dendrites of the horizontal axo-axonic cells were restricted to stratum oriens and ran parallel with the layers for several hundred micrometers. Single action potentials elicited by depolarizing current steps in these cells were often followed by a fast- and medium-duration afterhyperpolarization, distinguishing them from fast-spiking interneurons. In two out of four cells, trains of action potentials showed prominent early spike frequency adaptation and a characteristic "accommodative hump." Excitatory postsynaptic potentials (EPSPs) could be evoked by stimuli delivered to stratum oriens. Paired recordings unequivocally confirmed direct synaptic inputs from CA1 pyramidal cells. The kinetics of the EPSPs were fast (rise time 1.7 ± 0.6 ms, mean ±SD, n = 3; decay time constant 19.3 ± 2.4 ms). They showed paired-pulse depression with inter-stimulus intervals of 10–50 ms. One pair showed a reciprocal connection establishing a direct feedback loop. The axo-axonic cell-evoked inhibitory postsynaptic potentials (IPSPs) were reliable (failure rate ~10%). Our data show that the laminar distribution of the dendrites of axo-axonic cells can vary, suggesting distinct synaptic inputs. However, this remains to be shown directly, and we cannot exclude the possibility that all axo-axonic cells may gather similar synaptic input, leaving them as one distinct class of interneuron.**


**KEY WORDS: hippocampus; interneuron; GABAergic; inhibition; EPSP**

## INTRODUCTION

Hippocampal interneurons, although far outnumbered by pyramidal cells (Woodson et al., 1989; Aika et al., 1994), show great diversity (for review, see Freund and Buzsaki, 1996). Attempts to identify and classify the hippocampal interneurons relied on physiological properties (e.g., firing characteristics), the expression of molecular markers (e.g., calcium binding proteins or neuropeptides), or the extent of their dendritic and axonal arbors. The latter features point to an ordering principle, in which the functional location of a cell in a network may be demonstrated by the laminar location of its soma, dendrites, and axonal arbor (Somogyi et al., 1998). Because different pathways in the hippocampus are largely confined to specific layers, the laminar extent of the dendritic tree gives a first indication of the potential synaptic afferents to a given cell. Conversely, the functional output of a cell type within the hippocampal network depends primarily on its axonal target profile: interneurons making synapses only on the dendritic domain may modulate the integrative properties of pyramidal cells, whereas those targeting the somatic and perisomatic membrane are well situated to shape their firing patterns.

The target selectivity of axo-axonic cells is one of the best-defined organizational patterns among interneurons. This cell type is known to innervate almost exclusively axon initial segments of pyramidal cells (Somogyi, 1977; Somogyi et al., 1983). In the CA1 subfield of the hippocampus, their somata were described as located in stratum pyramidale; they typically have a radial dendritic tree spanning all layers with a prominent tuft in stratum lacunosum-moleculare (Somogyi et al., 1985; Buhl et al., 1994; Freund and Buzsaki, 1996; Pawelzik et al., 2002). Such a pattern predicts access to afferent synaptic input from all major known afferents, namely, the entorhinal, thalamic, CA1, and CA3 pyramidal glutamatergic inputs. However, none of these has been demonstrated directly to form synapses with axo-axonic cells in any species. In the present report, we describe identified axo-axonic cells with horizontal dendrites restricted exclusively to stratum oriens, where most CA1 pyramidal local axon collaterals make synapses with interneurons as well as pyramidal cells (Ramon y Cajal, 1893; Lorente de Nó, 1934; Buhl et al., 1994; Blasco-Ibanez and Freund, 1995; Ali and Thomson, 1998). In addition, we report the intrinsic membrane properties and characterize the synaptic responses of horizontal axo-axonic cells. Our results extend a functional taxonomy of interneurons based on a definition of their location in the network and a physiological characterization of their pre-and postsynaptic contacts.

[1]**MRC Anatomical Neuropharmacology Unit, Oxford University, United Kingdom** [2]**University Laboratory of Physiology, Oxford University, United Kingdom**
This research was made possible by support from an EC Framework V grant, the Royal Society, and Grant sponsor: Medical Research Council (UK); Grant sponsor: The Wellcome Trust; Grant number: 047313/Z/96.
Peter Szücs is currently at the Department of Anatomy, Histology, and Embryology, University of Debrecen, Debrecen, Hungary.
*Correspondence to: Paul Ganter, Current address: Centre for the Biology of Memory, NTNU, 7489 Trondheim, Norway. E-mail: paul.ganter@cbm.ntnu.no
Accepted for publication 3 April 2003
DOI 10.1002/hipo.10170

## MATERIALS AND METHODS

### Slice Preparation

Hippocampal slices were prepared as described earlier (Pike et al., 2000). All procedures were carried out in accordance with the UK Animals (Scientific Procedures) Act, 1986, and institutional guidelines. Briefly, young (P12–P16) Wistar rats (Harlan, UK) were deeply anesthetized with isoflurane (Isofane, Vericore, Marlow, UK) and subsequently decapitated. The brain was removed and placed in ice-cold artificial cerebrospinal fluid (ACSF) saturated with 95% $O_2$/5% $CO_2$. The ACSF contained (in mM): 126 NaCl, 3 KCl, 1.25 $NaH_2PO_4$, 2 $MgSO_4$, 2 $CaCl_2$, 26 $NaHCO_3$, and 10 glucose; pH 7.2–7.4. After removal of the frontal part of the brain and the cerebellum, horizontal slices (300 μm) were cut through the hippocampus with a microtome (Leica VT1000S, Leica, Nussloch, Germany). Immediately after sectioning, the slices were transferred to a holding chamber and were incubated in ACSF (as above) at room temperature (20–24°C). They were allowed a recovery period of ≥1 h before recording.

### Electrophysiological Recordings

The slices were transferred one by one to the recording chamber, which was continuously perfused with oxygenated ACSF at room temperature. Horizontal interneurons in stratum oriens were selected visually by aid of infrared (IR) differential interference contrast video microscopy (Sakmann and Stuart, 1995), on the basis of the horizontal orientation of their cell bodies. Patch pipettes were pulled from standard-walled borosilicate tubing (Clark GC120F-10, Pangbourne, UK). The pipette solution contained (in mM): 110 K-gluconate, 40 HEPES, 2 MgATP, and 0.3 GTP, 4 NaCl (pH adjusted with 1 M KOH to 7.2–7.3). Biocytin (5 mg/ml) was added to the pipette solution to permit identification of the recorded cells. Final osmolarity was ~300 mOsm. We used patch pipettes with a resistance of 6–10 MΩ corresponding to a tip diameter of ~1 μm. Patching was done using the "blow and seal" technique (Stuart et al., 1993). Whole-cell current-clamp recordings were made with an AxoClamp-2A amplifier (Axon Instruments, Union City, CA) in bridge mode. Capacitance compensation was maximal and bridge balance adjusted (~30 MΩ) during recording. For the synaptically connected pairs, the pipette solution contained (in mM): 126 K-gluconate, 10 HEPES, 4 MgATP, 0.3 NaGTP, 4 KCl, and 10 $Na_2$-phosphocreatine with 5 mg/ml biocytin added (pH adjusted to 7.2). The composition of the ACSF was similar to that above, except for a higher $CaCl_2$ concentration (i.e., 3 mM). The pyramidal cell was recorded using an Axopatch-1D amplifier (Axon Instruments) and the interneuron with an EPC7 amplifier (List, Germany).

For extracellular stimulation, patch pipettes with a tip diameter of ~2 μm, filled with ACSF, were used. Once a horizontal interneuron was selected, the stimulation electrode was placed on its subicular side in the outer third of stratum oriens. Stimulation was made with 50-μs-long constant-current pulses controlled by a Master-8 stimulator (AMPI, Jerusalem, Israel). After patching the interneuron and obtaining the whole-cell configuration, the stimulation intensity was gradually increased until synaptic responses were consistently evoked. During experiments, paired-pulse stimulation was used with an inter-stimulus interval of 50 ms, every 5 s. The membrane potential was kept constant within a range of −65 mV and −70 mV throughout the experiment, via DC current injection through the patch pipette. Extracellularly evoked excitatory postsynaptic potentials (EPSPs) were recorded with 5 μM bicuculline methochloride added to the ACSF to block γ-aminobutyric acid $(GABA)_A$ receptor-mediated inhibition.

In one of the paired recordings (cell 081298), the axo-axonic cell was held under voltage clamp at a holding potential of −60 mV, while triplets of action potentials were evoked in the presynaptic pyramidal cell with interspike intervals of 25 ms. Series resistance was not compensated during voltage clamp.

### Data Acquisition and Analysis

The data were low-pass filtered at 3 kHz and were acquired at a sampling rate of 5 kHz. The slight deviation from the Nyquist sampling requirement had no significant effect on the measures analyzed in the present study. All subsequent analysis was done using custom-made procedures in Igor Pro software (Lake Oswego, OR). The membrane time constant (τ) and input resistance ($R_{in}$) were determined by fitting the sum of one decaying and one rising exponential function to the cells' voltage response to small negative current steps (−10 pA, 200 ms). This was done to ensure acceptable fits in the presence of a sag toward the baseline in the voltage trace. The decaying function was then used to estimate τ. Similarly, $R_{in}$ was calculated as the asymptotic amplitude of the decaying exponential function divided by the amplitude of the current step. Action potential and afterhyperpolarization (AHP) amplitudes were measured from the action potential threshold, which was detected by a maximum in the second derivative of the voltage trace. The width of the action potentials was determined at half-peak amplitude measured from threshold.

Measurements of synaptic potentials (excitatory postsynaptic potentials [EPSPs] and inhibitory postsynaptic potentials [IPSPs]) and currents (excitatory postsynaptic currents [EPSCs]) were made with a procedure similar to that described by Feldmeyer et al. (1999). Briefly, their amplitudes were measured as the difference between the peak amplitude in a pre-defined window after the stimulation artifact or presynaptic action potential and the mean amplitude in a 1-ms time window just preceding the artifact or action potential. The background noise was estimated in the same way from the prestimulus baseline, time windows shifted by 20 ms. The latency of the synaptic event was determined as the first intersection between the baseline and a parabola fitted to the rising phase (20–80%) of the EPSP. The decay time constant ($\tau_{decay}$) was estimated from a single exponential function fitted to the decay phase of the respective synaptic response. The paired-pulse ratio was calculated from the average EPSPs of 300 consecutive sweeps, unless indicated otherwise. The average excitatory response was obtained by aligning individual traces with respect to the peak of the first action potential in the pyramidal cell in the case of paired recordings, or to the first stimulation artifact in the case of extracellular stimulation. Response failures were judged to have oc-

curred, if the amplitude of the EPSP was within 2 SD of the noise distribution. The spike triggered average of the IPSP was determined using 100-ms time windows, starting 15 ms before each action potential in the axo-axonic cell. All curve fits were done using the built-in iterative Levenberg-Marquardt algorithm in Igor Pro. Statistical significance was assessed using Student's *t*-test.

## Histological Processing

During recording, the cells were filled with biocytin and were subsequently processed using standard procedures; two cells were processed only for light microscopic analysis and two cells for combined light and electron microscopic analysis. Briefly, slices for light microscopic analysis alone were fixed in a solution containing 4% paraformaldehyde and ~0.2% picric acid in 0.1 M phosphate-buffered saline (PBS; pH 7.4) and stored at ~4°C. Several days later, they were washed thoroughly in 0.1 M phosphate buffer (PB), then in 0.3% $H_2O_2$ in Tris-buffered saline (TBS), followed by a rinse in TBS. Then the slices were incubated in a solution of avidin-biotinylated horseradish peroxidase (HRP) complex (ABC; Vector Laboratories, Burlingame, CA) in TBS, containing 0.3% Triton. Peroxidase activity was visualized by incubation for 5 min in 0.05% 3,3′-diaminobenzidine tetrahydrochloride (DAB) in TB (pH 7.6) followed by another 10 min in DAB containing 0.01% $H_2O_2$. After more extensive washing, first in TB, then in 0.1 M PB, slices were treated with 0.5% $OsO_4$ in 0.1 M PB for 5–10 min before they were washed in PB, dehydrated, and finally permanently mounted in Durcopan resin (Fluka; Sigma-Aldrich, Gillingham, UK) on glass slides under a coverslip. As most synaptic boutons on axon initial segments of pyramidal cells in the CA1 area have been shown to be immunopositive for parvalbumin (Katsumaru et al., 1988), no further immunohistochemical testing of the cells was carried out.

Slices for light and electron microscopy were fixed in 4% paraformaldehyde, 0.05% glutaraldehyde, and ~0.2% picric acid in 0.1 M phosphate buffer (pH 7.4). The slices were resectioned at 60-μm thickness and processed as described earlier (Maccaferri et al., 2000). No detergent was used during processing; the sections were contrasted with aqueous uranyl acetate; 1% $OsO_4$ was used for postfixation. The sections were permanently mounted in Durcopan resin, as described above. The axonal and dendritic trees of each neuron were analyzed at high magnification, using an oil immersion objective (×100). Two of the recovered cells were subsequently reconstructed using a light microscope with ×40 objective and a drawing tube.

For electron microscopy, axon-rich areas, including all layers covered by the axonal field, were cut out from the thin layer of resin on the slide and re-embedded for further sectioning at ~70-nm thickness. Serial electron microscopic sections were cut and mounted on single-slot pioloform-coated copper grids and contrasted with lead citrate. The sections were scanned in the electron microscope, and all biocytin-filled axonal profiles that formed synaptic junctions were photographed. Since all profiles were followed and the plane of the section randomly cut through the axonal branches, the above procedure ensured a random sample of postsynaptic targets and provide an objective basis for cell classification (Somogyi et al., 1998). Postsynaptic elements were identified on published criteria (Peters et al., 1991). In brain slices incubated in vitro, some structural features change with incubation time, and axon initial segments (AIS) were identified as described before (Maccaferri et al., 2000). The two axonal trees sampled in this study were in slices with excellent preservation, and the vast majority of AIS were easily identified. All chemicals and drugs were purchased from Sigma (St. Louis, MO) and Tocris (Bristol, UK).

# RESULTS

From a total of 57 successfully recovered and identified stratum oriens horizontal interneurons, four were judged to be axo-axonic cells based on their axonal arborization. This was determined in an initial light microscopic analysis, giving them a "chandelier"-like appearance (Somogyi, 1977; Somogyi et al., 1985; Buhl et al., 1994) (Fig. 1A,E). Electron microscopic analysis of a random sample of the postsynaptic targets of two of these cells provided unequivocal evidence that this prediction was correct. The following discussion presents a detailed analysis of the properties of these cells. Some of the physiological features are summarized in Table 1.

## Axonal and Dendritic Patterns; Synaptic Targets

All four cells presented in this report shared the main anatomical feature of a characteristic axonal arbor located primarily in the part of stratum pyramidale adjoining stratum oriens and also in stratum oriens itself (Fig. 1A,E). For two of the cells (cell 240499 and 080299), some bouton-bearing axon collaterals also spread into the deep stratum oriens and alveus. Only a few collaterals penetrated the compact layer of stratum pyramidale and stratum radiatum, but when they did, they established radially oriented rows of boutons, the hallmark of axo-axonic cells (Fig. 1A,E). Because of the truncation of axonal trees by the slicing procedure, no attempt was made to count the rows of boutons here. The main axons of horizontal axo-axonic cells originated in the soma in three cases and from a very proximal dendrite in one case.

Electron microscopic analysis of a random sample of 10 postsynaptic targets for each of cell 081298 and 080299 showed that they made synapses exclusively on axon initial segments. Even when the identified bouton was in direct membrane apposition to the cell body of a pyramidal cell, it made no synaptic junction with it, but formed a junction with a nearby AIS. The AIS were recognized by their higher electron opacity than that of dendrites in the same material, and, when present, the electron-dense membrane undercoating, microtubule fascicles, and a high density of membranous tubules and large vesicles (Fig. 1F). They only received type II synapses both from the recorded axo-axonic cell and from unlabeled boutons, presumably originating in other converging axo-axonic cells (Fig. 1F). These axon initial segments very likely originate in CA1 pyramidal cells, although only three could be followed back to the parent cells within the examined series of sections. The axons did not form appositions with the axon initial segment, soma, or dendrite of the labeled interneurons themselves; therefore, there was no indication of autaptic contacts (Cobb et al.,

1997). The axon initial segment of interneurons examined in the rodent hippocampus so far received no synapses, or very few (P. Somogyi, unpublished observation).

The soma of all four cells was spindle shaped, elongated parallel with the layers (called the horizontal orientation), with short and long axes of ~10 and 20 μm, respectively. Three of the somata were located in stratum oriens about halfway between the stratum pyramidale and the alveus (Fig. 1A–C); one was closer to the alveus. The recovery of three of the cells was excellent, and we were able to trace dendrites to their apparent natural ends. One of the cells showed signs of collapse, and the dendrites were filled with HRP reaction product only in patches. Nevertheless, some could be traced up to a 200-μm distance, and it is unlikely that any major dendrite was missed. Most dendrites emanated from the two poles of the soma and ran parallel with the pyramidal cell layer. Branching occurred mainly at the origin of dendrites and in their most distal parts. The dendrites showing natural ends could be traced for up to ~340 μm from the soma, making a total lateral dendritic extent of 400–500 μm. The dendrites were mostly smooth, with a few filopodial extensions, as is typical in young animals, and with a low density of drumstick-shaped spines on two of the cells. Some dendrites emanated from the sides or upper parts of the soma and were truncated by the slicing procedure. We cannot exclude the possibility that some of the truncated dendrites extended into layers outside the stratum oriens, but this was observed only in one of the cells (cell 240499), which had a small dendrite reaching the lower part of stratum radiatum.

## Intrinsic Membrane Properties

We characterized the physiological properties of the cells in control ACSF immediately after whole-cell configuration was obtained. To determine the intrinsic membrane properties at rest, a series of step currents of varying amplitude was applied. The input resistance of the cells ($R_{in}$) was 217 ± 34 MΩ (n = 4) and the time constant ($\tau_{cell}$) 23 ± 7 ms (Table 1 and Fig. 2A). Voltage sag was not observed, either with depolarizing or with hyperpolarizing current steps in the range of ±15 mV from rest. Small suprathreshold current steps (60 pA) elicited short-lasting, overshooting action potentials, followed by a succession of a fast AHP, an afterdepolarization (ADP), and a weak medium duration AHP; the latter two, however, were not always clearly present. When the current step amplitude was increased to ~100 pA, two of the neurons fired action potential trains with an "accommodative hump" (Cauli et al., 2000) (Fig. 2B). By accommodative hump, we refer to a characteristic succession of a decrease of the action potential overshoot followed by a gradual increase to a steady-state level, mirrored by a similar increase and subsequent decrease of the firing threshold. This decrease in action potential amplitude occurred within ~50 ms after the first action potential of a train coinciding with a prominent early spike frequency adaptation, after which the neurons fired at a fairly constant rate (Fig. 2B–D).

## Synaptic Properties

We characterized the properties of excitatory synaptic inputs evoked by extracellular stimulation in stratum oriens in detail in one cell (Table 2 and Fig. 3). After application of bicuculline methochloride (5 μM), EPSPs were elicited every 5 s. The EPSP amplitudes showed an extensive trial-to-trial variability (Fig. 3A,C), but remained stationary within the recording period of 25 min (Fig. 3C). On average, they were 3.2 ± 2.0 mV in amplitude for EPSP1 and 2.8 ± 1.6 mV for EPSP2 (mean ± SD, n = 300; $P < 0.01$, *t*-test), recorded at −67 mV membrane potential. Thus, the cell showed paired-pulse depression (paired-pulse ratio: 0.86). There was no correlation between the amplitudes of EPSP1 and EPSP2 in individual sweeps ($r^2 = 0.01$; n = 300) (Fig. 3D). The latency was not significantly different between EPSP1 and EPSP2 ($P > 0.6$; *t*-test, n = 300), suggesting that the difference in amplitude was not due to the activation of different sets of afferents. None of the latency, rise time, half-width, or decay time constant showed a correlation with EPSP amplitudes (all $r^2 < 0.08$). The distribution of latencies was close to normal and could be fitted by a single Gaussian function (Fig. 3F). The distribution of the rise times was slightly skewed to the right. The apparent failure rate under our conditions was very low, less than 5% for both EPSP1 and EPSP2. The source of the presynaptic axons was not identified in these experiments, but the most frequent glutamatergic axons at the location of the stimulating electrode derive from CA3 and CA1 pyramidal cells.

Paired recordings unequivocally confirmed monosynaptic connection between CA1 pyramidal cells and horizontal axo-axonic cells in stratum oriens (Fig. 4A,B). In one axo-axonic cell (cell 081298), single unitary EPSPs had an average amplitude of just over 1 mV (average of 60 consecutive sweeps, not shown), with individual responses of up to ~2.5 mV. The kinetic properties of the unitary EPSPs were not different from those evoked by extracellular stimulation (cf. Table 2). In another cell (cell 080299), EPSCs were recorded. Individual responses showed considerable variability with respect to their latency and rise time (Fig. 4B). The estimated kinetic properties of individual EPSCs whose amplitude exceeded 25 pA during stationary conditions (first 65 responses) were: rise time, 3 ± 2 ms; half-width, 4 ± 2 ms; and decay time constant, 5 ± 2 ms. In both pairs, a succession of three action potentials in the presynaptic pyramidal cell at frequencies of 25–100 Hz revealed short-term depression of the synaptic responses.

In one of the paired recordings (cell 081298), we found a reciprocal connection from the axo-axonic interneuron to the CA1 pyramidal cell (Fig. 5A). Trains of action potentials in the axo-axonic cell very reliably evoked IPSPs in the pyramidal cell (failure rate ~10%). Individual IPSPs were up to 1.3 mV in amplitude at −56 mV membrane potential. They had short latencies (~1 ms), showed short-term depression, and their mean amplitude decreased with increasing firing frequency in a train of presynaptic action potentials (Fig. 5B). This is, to our knowledge, the first reciprocal connection reported between an axo-axonic and a pyramidal cell.

# DISCUSSION

We analyzed identified axo-axonic cells with horizontally oriented dendrites restricted to the stratum oriens in the hippocampal

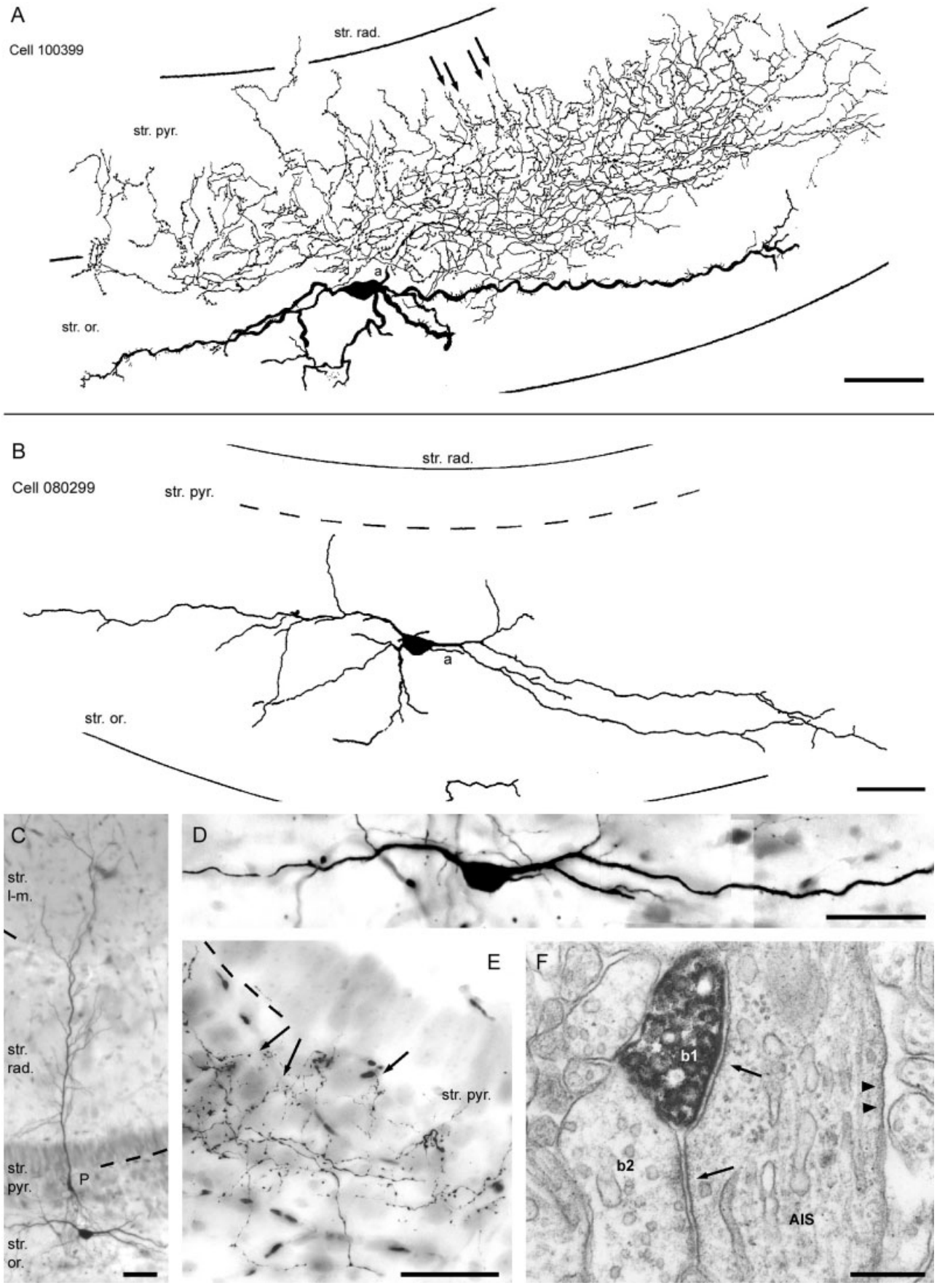
A
Cell 100399
str. rad.
str. pyr.
a
str. or.
B
Cell 080299
str. rad.
str. pyr.
a
str. or.
C
str.
l-m.
str.
rad.
str.
pyr.
P
str.
or.
D
E
str. pyr.
F
b1
b2
AIS

**FIGURE 1**

*TABLE 1.*

*Membrane Properties of Horizontal Axo-axonic Cells*

| | Code (age) | | | |
|---|---|---|---|---|
| | 100399 (P15) | 240499 (P16) | 081298 (P12) | 080299 (P14) |
| Time constant (ms) | 19 | 16 | 25 | 32 |
| Input resistance (MΩ) | 186 | 189 | 240 | 252 |
| AP amplitude (mV) | 71.4 | 72.3 | 75.1 | 90.2 |
| AP overshoot (mV) | 25.2 | 33.9 | 32.8 | 52.0 |
| AP width (ms) | 1.0 | 0.7 | 1.0 | 1.1 |
| fAHP amplitude (mV) | 6.0 | 12.7 | 12.1 | 13.7 |

AP, action potential; fAHP, fast afterhyperpolarization.

CA1 area. The laminar selectivity of their dendrites and the target profile of their axonal arborization might predict how they are embedded in the CA1 network; therefore, we compare these cells with previously described interneurons.

## Interneurons and Afferents in Stratum Oriens

The confinement of the dendritic tree to the stratum oriens was rather surprising, as horizontal orientation of dendrites and the restriction to one or two specific layers has generally been considered a characteristic of interneurons innervating pyramidal cell dendrites, perisomatically terminating cells having radial dendritic trees, usually spanning all layers (Freund and Buzsaki, 1996). Although it cannot be absolutely excluded that radially running dendrites were cut or not filled, this seems unlikely, as the degree of staining was generally excellent. Reports of horizontal interneurons in stratum oriens of the CA1 area, with axons selectively terminating in the strata pyramidale and oriens, are neither new (Sala, 1891; Ramon y Cajal, 1893; Kölliker, 1896; Lorente de Nó, 1934) nor uncommon (Lacaille et al., 1987; McBain et al., 1994; Parra et al., 1998; Fukuda and Kosaka, 2000). As most synaptic boutons on axon initial segments of pyramidal cells in the CA1 area

**FIGURE 1. Identification of horizontal axo-axonic cells. A: Reconstruction of a cell showing dendrites (thick processes) running mainly parallel with the layers in stratum oriens (str. or.) and axonal arbor mostly in the deep pyramidal layer (str. pyr.) and adjacent stratum oriens. Note the characteristic radial axonal terminal segments (arrows) defining it as an axo-axonic cell. Some shrinkage is likely to have occurred during the histological processing, which is apparent from the undulating appearance of the dendrites. B: Reconstruction of the dendritic tree of another cell also shown in C–F. The broken line denotes the compact sublayer of stratum pyramidale, as also seen in the micrograph shown in E. C: Light micrograph of the same cell shown together with a reciprocally connected pyramidal cell (P). The reciprocal connection was evident from the synaptic responses (Figs. 4A and 5). D: Light micrograph of the horizontally elongated soma and dendritic tree. E: Characteristic axonal segments (arrows) in the deep pyramidal layer. F: Electron micrograph of one of the boutons of this cell (b1) establishing a type II synapse (upper arrow) with an axon initial segment (AIS). The latter is identified by the electron-opaque membrane undercoating (arrowheads). Another unlabeled bouton (b2), presumably from a converging axo-axonic cell also makes a type II synapse (lower arrow) with the same axon. a, main axon of the cells, str. rad., stratum radiatum; str. l-m., stratum lacunosum-moleculare. Scale bars = 50 μm in A–E; 0.2 μm in F.**

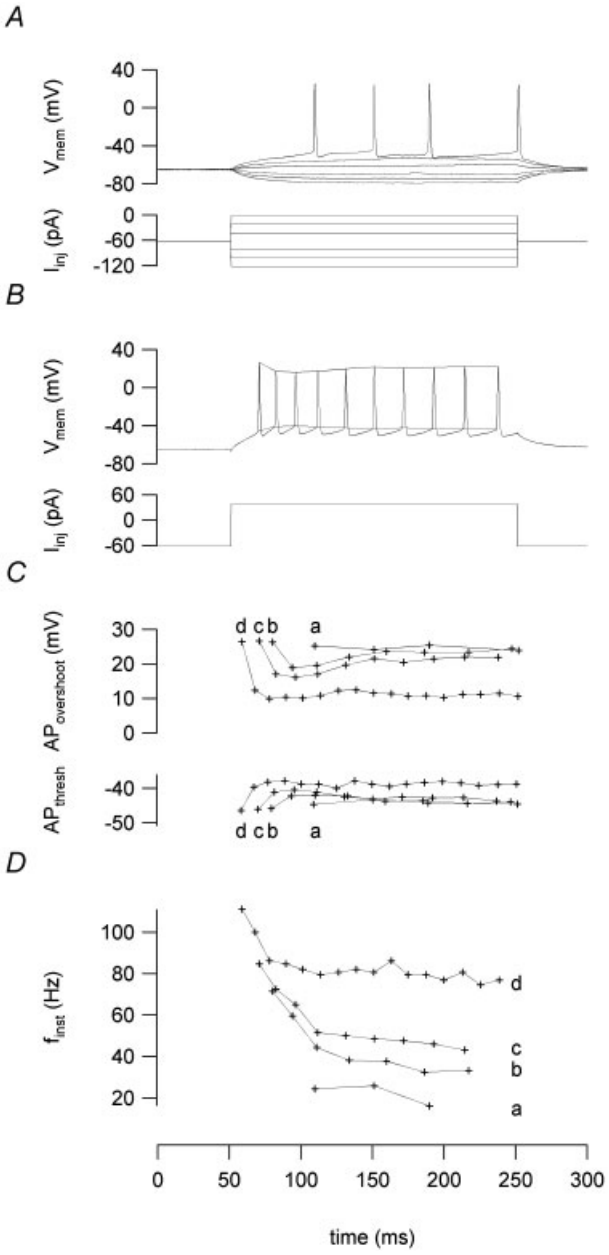


**FIGURE 2. Characterization of intrinsic properties of an identified axo-axonic cell (cell 100399). A: Voltage response (upper panel) to a series of current steps (lower panel). Note the curved trajectory of the membrane potential after the fast afterhyperpolarization. However, the medium duration afterhyperpolarization was not very prominent in this cell. B: Train of action potentials in response to a 100-pA current step; note the accommodative hump and early spike frequency adaptation. C: Action potential overshoot and action potential threshold for step currents of a: 60, b: 80, c: 100, and d: 200 pA. Note that the accommodative hump is only apparent at medium average firing rates. D: Instantaneous firing frequency as a function of step current amplitude (same stimulation intensities as in C).**

*TABLE 2.*

*Properties of EPSPs Elicited in Axo-axonic Cells*

| | Extracellular stim. 1[a] (100399) | | Extracellular stim. 2[b] (240499) | | Paired recording 1[c] (081298) |
|---|---|---|---|---|---|
| | EPSP1 | EPSP2 | EPSP1 | EPSP2 | Single EPSPs |
| Amplitude (mV) | 3.2 ± 2.0 | 2.8 ± 1.6 | 2.2 | 3.6 | 1.2 |
| 20–80% rise time (ms) | 1.5 ± 0.6 | 2.0 ± 1.3 | 2.1 | 1.8 | 1.2 |
| Half-width (ms) | 16.6 ± 4.8 | 18.5 ± 6.7 | 21.9 | 18.1 | 21.5 |
| Decay time constant (ms) | 18.6 ± 6.7 | 20.9 ± 8.2 | 23.8 | 26.0 | 22.0 |

EPSP, excitatory postsynaptic potential.
[a]Mean ± SD; n = 300.
[b]Measured from analogue averages of 100 consecutive sweeps.
[c]Measured from analogue averages of 60 consecutive sweeps.

have been shown to be immunopositive for parvalbumin (Katsumaru et al., 1988), axo-axonic cells might have been included among the parvalbumin-positive ($PV^+$), horizontal interneurons that have been described in stratum oriens (Kosaka et al., 1987; Fukuda and Kosaka, 2000). However, the precise identity and synaptic targets of these cells were not evaluated. So far, all confirmed hippocampal axo-axonic cells were reported to have main dendrites crossing through stratum radiatum with only little branching, and terminating in a characteristic dense tuft in stratum lacunosum-moleculare, in addition to smaller basal dendrites in stratum oriens/alveus, similar to the dendritic extent of pyramidal cells (Li et al., 1992; Buhl et al., 1994). Two axo-axonic cells in stratum pyramidale of the CA3 area described by Gulyas et al. (1993) (AA1, and AA2) had "dendrites in a horizontally elongated field, primarily in stratum oriens." However, the dendrites of these cells descended radially, similar to basal dendrites of pyramidal cells; in this area, all known glutamatergic afferents that innervate stratum oriens innervate stratum radiatum as well.

To date, synaptic inputs to axo-axonic cells have not been demonstrated directly, beyond the position of their dendrites. The laminar specificity of the dendritic arbor of hippocampal interneurons provides only a first indication as to their possible afferents. Because the local axon collaterals of pyramidal cells in the CA1 area are distributed mainly in stratum oriens, the dendritic restriction to stratum oriens suggests that local pyramidal cells might provide the primary excitatory input. Thus, these axo-axonic cells could be involved in local feed-back circuits, like other horizontal interneurons in stratum oriens (Maccaferri and McBain, 1995; Blasco-Ibanez and Freund, 1995; Katona et al., 1999). Our paired recordings unequivocally confirmed both the direct synaptic input from local pyramidal cells and the involvement in a feedback loop. In contrast, based on the aforementioned vertical dendritic arborization, Li et al. (1992) suggested that the axo-axonic cells receive their main synaptic inputs from entorhinal afferents in stratum lacunosum-moleculare, as well as being recurrently activated by local pyramidal cells. Since some entorhinal afferents terminate in stratum oriens (Deller et al., 1996), this could also be the case for horizontal axo-axonic cells. Even though entorhinal afferents might be not as numerous as local pyramidal axon collaterals in stratum oriens, it cannot be excluded that horizontal axo-axonic cells attract entorhinal inputs in the same relative proportion as radial ones.

Other previous reports suggested that axo-axonic cells receive synaptic inputs from all major afferent pathways (Buhl et al., 1994). The two additional known glutamatergic inputs terminating in the dendritic layer of horizontal axo-axonic cells are the Schaffer collateral/commissural afferents and afferents from the amygdala (Pikkarainen et al., 1999). Inputs have also been suggested from local interneurons (Katsumaru et al., 1988; Buhl et al., 1994), especially from $PV^+$ basket cells in stratum oriens (Sik et al., 1995); see also (Fukuda et al., 1996; Fukuda and Kosaka, 2000), and possibly also from extrahippocampal afferents (Freund and Antal, 1988; Freund et al., 1990; Gulyas et al., 1990; Freund, 1992; Fukuda et al., 1996). None of these suggestions has been tested directly. Based on the dendritic location, we cannot rule out any of these inputs to horizontal axo-axonic cells. Finally, $PV^+$ cells in stratum oriens, including those with horizontal dendrites, have been demonstrated to form dendritic gap junctions (Fukuda and Kosaka, 2000), the structural correlate of electrical coupling. Because the axonal targets were not identified, it remains to be investigated whether they included axo-axonic cells like those presented in this study.

The Schaffer collateral/commissural input to the CA1 area deserves closer scrutiny, because, depending on the proximodistal position of the CA3 pyramidal cells relative to the CA1 area, the cells innervate different sublayers (Ishizuka et al., 1990; Li et al., 1994). The CA3 pyramidal cells most proximal to the CA1 area innervate stratum oriens almost exclusively, thus matching the CA1 pyramidal local collaterals. It cannot be excluded that these CA3 pyramidal axons innervate different sets of interneurons from those innervating either both stratum radiatum and oriens or only stratum radiatum, as the most distal CA3 pyramidal neurons do. It is interesting that, in addition to the axo-axonic cells presented in this report, at least four other classes of axonally defined cells, CCK-positive basket cells (Maccaferri et al., 2000; Pawelzik et al., 2002), $PV^+$ basket cells (Pawelzik et al., 2002), bistratified cells

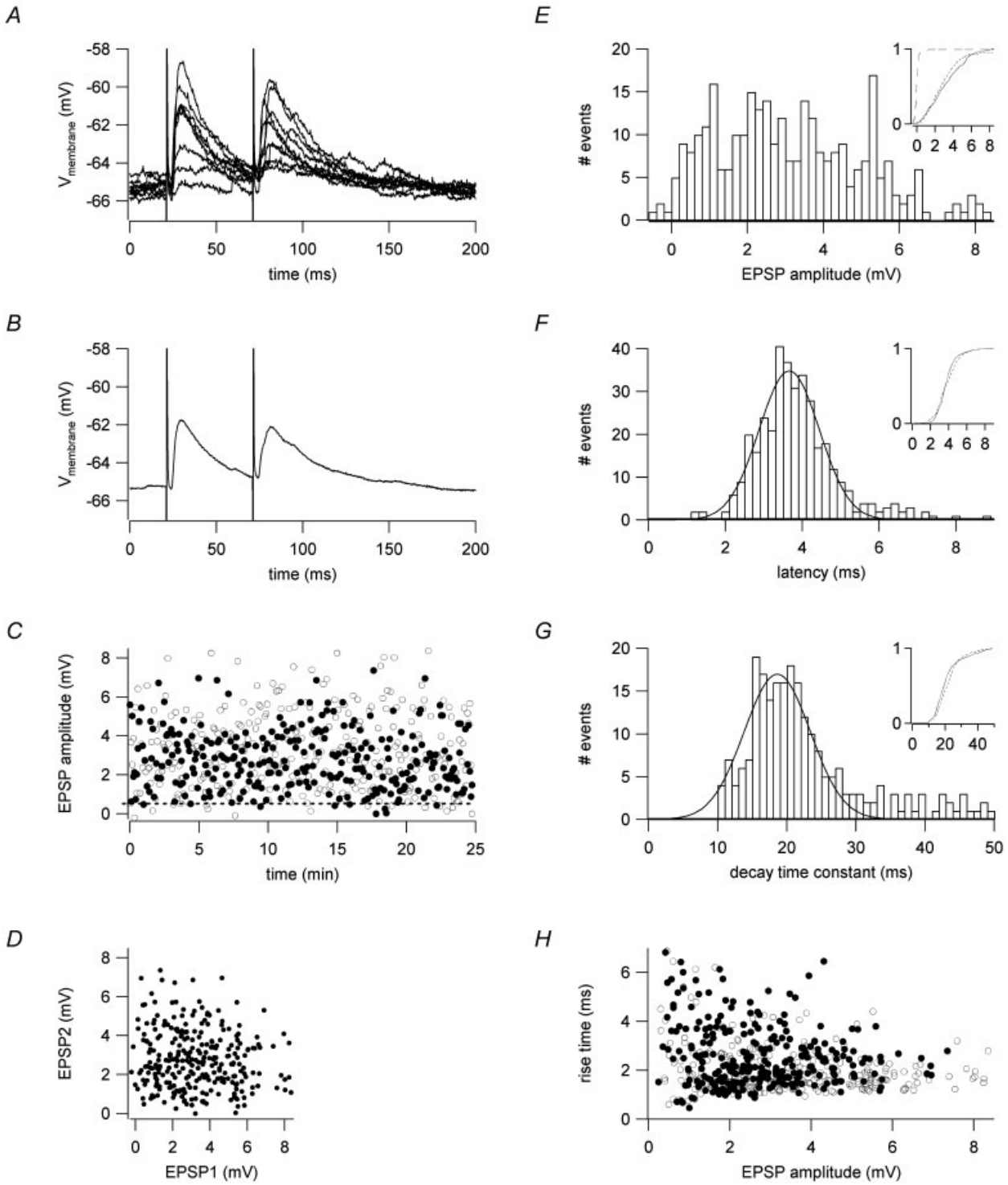


**FIGURE 3. Characterization of excitatory postsynaptic potential (EPSP) properties in an axo-axonic cell (cell 100399). A: Ten consecutive EPSPs elicited by paired-pulse extracellular stimulation (50-ms interval). Note the relatively large variability and lack of response failures. B: Average EPSP (n = 10) showing slight paired-pulse depression. C: EPSP peak amplitude plotted over time (open circles, first EPSP; filled circles, second EPSP) showing large fluctuations of individual responses and only few response failures. The response remains stationary over the recording epoch. The dotted line indicates +2 SD of the noise distribution. D: Scatter plot of peak amplitudes of the second EPSP (EPSP2) versus the first EPSP (EPSP1). No correlation was seen between EPSP1 and EPSP2 ($r^2 < 0.01$, n = 300). E: Amplitude histograms of EPSP1 from the same time epoch (bin width, 0.2 mV); inset, cumulative histograms including noise distribution. There is a clear separation of response distribution from the noise distribution (solid line, first EPSP; dotted line, second EPSP; broken line, noise). F: Distribution of the latency of the first EPSP (bin width, 0.2 ms) with superposed Gaussian fit; inset, cumulative histograms of latency of the first EPSP (solid line) and second EPSP (dotted line). G: Distribution of decay time constant of first EPSP (bin width, 1 ms) with superposed Gaussian fit; inset cumulative histogram of decay time constants of the first EPSP (solid line) and second EPSP (dotted line). H: Scatter plot of rise time versus peak amplitude of first EPSP (open circles) and second EPSP (filled circles).**

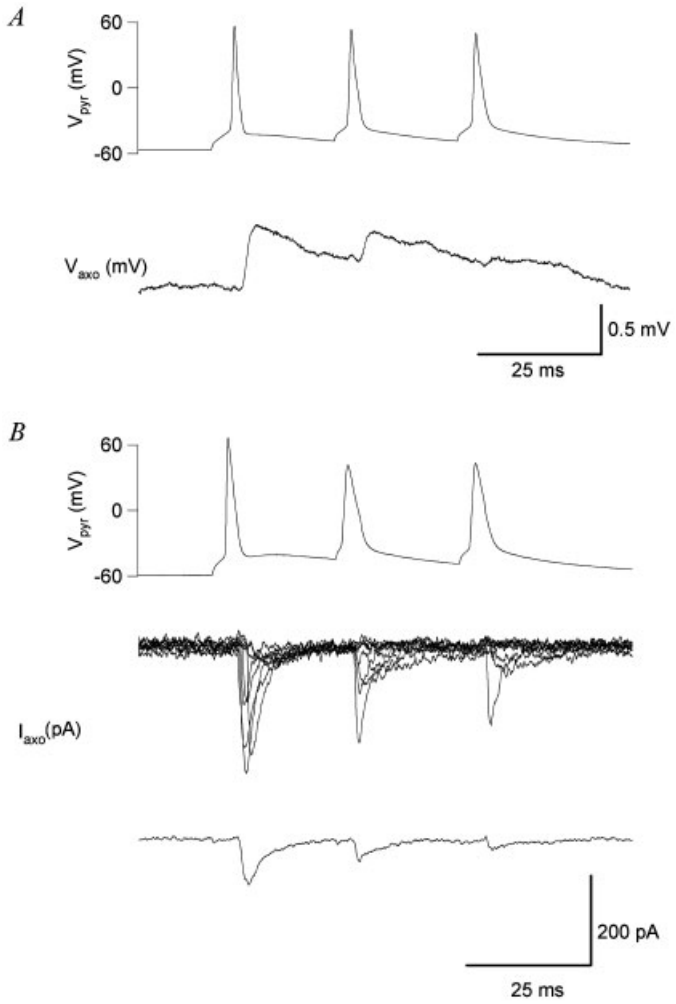


**FIGURE 4. Characterization of unitary excitatory responses in axo-axonic cells. A: Average of 60 consecutive action potential triplets in a CA1 pyramidal cell and the corresponding evoked excitatory postsynaptic potentials (EPSPs) (cell 081298). The unitary EPSPs look similar to those evoked with extracellular stimulation. The amplitudes of the EPSPs presented here were smaller than those evoked using single stimuli earlier in the experiment. B: Unitary excitatory postsynaptic currents (EPSCs) recorded in a different cell (cell 080299; individual responses and average). The individual traces were aligned on the peak of the first action potential. Both the EPSPs and EPSCs show short term depression at interspike intervals of 25 ms.**

(Maccaferri et al., 2000; Pawelzik et al., 2002), and O-LM cells (Oliva et al., 2000), have been found to have a subset in stratum oriens with horizontally oriented dendrites, and other sets in the other layers with radial dendrites. As it is unknown whether the subsets differ in their inputs, the possibility remains that they are in fact equivalent on the basis of input/output criteria, but the oriens/alveus region imposes a horizontal dendritic orientation during ontogenesis.

The target selectivity of neurons is an important factor for the network function of those cells. The cells recorded in this report share the characteristic axonal arborization pattern with previously recorded axo-axonic cells, suggesting that they target the axon initial segments of pyramidal neurons. For two of the cells this was verified by electron microscopic analysis. Direct evidence for recurrent regulation of their own input sources came from a reciprocally connected cell pair.

## Intrinsic Properties and Action Potential Firing

The time constant and input resistance of the cells recorded fall within the range reported by Zhang and McBain (1995a) for stratum oriens interneurons (200–600 MΩ). The firing of these horizontal axo-axonic cells showed two distinctive features. First, individual action potentials were often followed by triphasic afterpotentials (see Buhl et al., 1994; Morin et al., 1996; Cope et al., 2002). Second, trains of action potentials sometimes showed a characteristic temporal structure with prominent early spike frequency adaptation, followed by a rather constant steady-state firing. This early spike frequency adaptation coincided with a depolarizing wave, which has been called an accommodative hump

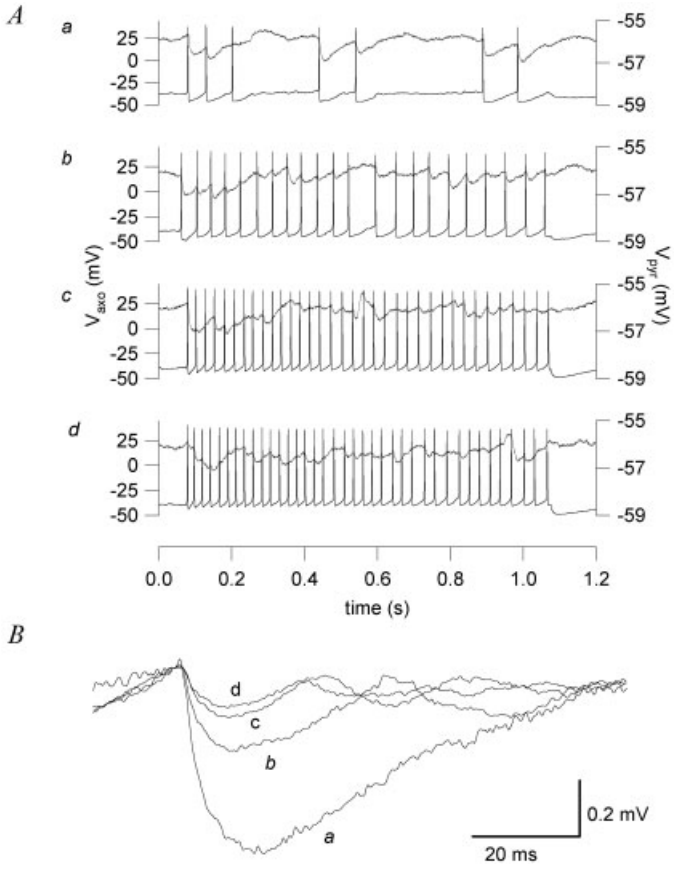


**FIGURE 5. Characterization of unitary inhibitory postsynaptic potentials (IPSPs) evoked by an axo-axonic cell (cell 081298). A: Trains of action potentials in the axo-axonic cell reliably evoked IPSPs in a CA1 pyramidal cell, which innervated the interneuron (same pair as in Fig. 4A). At frequencies above ~10 Hz the IPSPs showed depression. B: Spike triggered average IPSPs from the trains above, including apparent failures. The mean response amplitude gets smaller with higher frequency of presynaptic action potentials. Note that at higher frequencies, the average waveforms include consecutive IPSPs after the spike aligned IPSP. Average firing rates: a, ~7 Hz; b, ~22 Hz; c, ~35 Hz; d, ~38 Hz.**

(Cauli et al., 2000), also noticeable in the figures of Buhl et al. (1994). These features were not always clearly apparent and tended to disappear during longer recordings. We did not test whether this was an effect of bicuculline (Pedarzani et al., 2000; Savic et al., 2001) or reflected some change in the general condition of the cells.

Although previous descriptions commonly characterized interneuron firing by narrow action potentials with prominent AHPs, absence of ADPs, and high-frequency trains of action potentials with only weak spike frequency adaptation (Schwartzkroin and Kunkel, 1985; Lacaille et al., 1987; Lacaille and Schwartzkroin, 1988; Han et al., 1993; Zhang and McBain, 1995a), later studies described spike frequency adaptation in certain types of interneurons (Lacaille and Williams, 1990; Buhl et al., 1994; Mott et al., 1997; Chitwood and Jaffe, 1998), and even classified interneurons based on specific patterns of spike frequency adaptation (Gupta et al., 2000). More specifically, $PV^+$ cells, including some basket and axo-axonic cells (Katsumaru et al., 1988), have usually been associated with a fast-spiking phenotype (Kawaguchi et al., 1987; Kawaguchi, 1995; Kawaguchi and Kubota, 1997). However, more recent studies reported a wider variety of spiking patterns among hippocampal $PV^+$ interneurons (Pawelzik et al., 2002). The firing properties of the axo-axonic cells reported in this paper are consistent with the notion of a less homogeneous pattern of discharge of different interneuronal types than previously thought.

### Synaptic Properties

Extracellular stimulation in stratum oriens evoked EPSPs in axo-axonic cells, probably mainly via ortho- and/or antidromic activation of axon collaterals from CA1 pyramidal cells. Similar to EPSPs recorded in radially oriented axo-axonic cells (Buhl et al., 1994), the amplitudes of EPSPs evoked in this way showed a relatively large variability ($CV_{EPSP1} = 0.62$, $CV_{EPSP2} = 0.56$). The observed low failure rate is consistent with previous reports, showing that interneurons targeting the perisomatic domain respond reliably to excitatory synaptic inputs (Gulyas et al., 1993). However, in order to estimate the release probability at individual synaptic junctions, paired recordings with subsequent electron microscopic verification of the number of synaptic contacts would be necessary. The distribution of latencies and independence of rise time from EPSP amplitude suggest monosynaptic input from a small number of fibers. Both measures were very similar for EPSP1 and EPSP2. Thus, it is unlikely that any differences between EPSP1 and EPSP2 arose due to variations in the kinetics of the release machinery (see Waldeck et al., 2000) or to activation of different sets of fibers.

Paired recordings confirmed the direct input from CA1 pyramidal cells. A comparison of the properties of the unitary EPSPs with those evoked by field stimulation confirmed that they had almost identical kinetic properties and that their amplitudes were in the same range. This supports the view that our extracellular stimulation protocol activated a small number of collaterals from CA1 pyramidal cells. In both cases, the decay time constant of the EPSPs was comparable to the membrane time constant. They were similar to the synaptic properties reported for radially oriented axo-axonic cells (Buhl et al., 1994). The considerable variability of the latency and rise time of individual EPSCs (Fig. 4B) could be due to more than one synaptic contact between the pyramidal and the axo-axonic cell.

Three of the four horizontal axo-axonic cells displayed paired-pulse synaptic depression. This was likely to be due to a decrease in release probability, as suggested by an increase of synaptic failures. This is in contrast to the paired-pulse facilitation seen in a different class of horizontal interneurons in stratum oriens, the O-LM cells (Ali and Thomson, 1998), but consistent with paired-pulse depression in other interneurons targeting the perisomatic domain of pyramidal neurons (Ali et al., 1998).

The pyramidal cell innervated by one of the axo-axonic cells responded with IPSPs reliably at frequencies up to ~25 Hz. However, as this experiment was done at an elevated extracellular calcium concentration, it is currently unclear whether this reflects physiological release probabilities. With higher firing frequencies, the failure rate appeared to increase and the amplitude of individual IPSPs to decrease. As long as the firing patterns of axo-axonic cells in the intact network in vivo have not been established, it is difficult to assess the functional significance of the short-term dynamics of these synapses.

## CONCLUSIONS

Somata of axo-axonic cells have previously been localized primarily in the pyramidal cell layer. Other studies on interneurons in stratum oriens mainly found horizontal O-LM cells and radial basket cells (see Blasco-Ibanez and Freund, 1995; Zhang and McBain, 1995b; Ali et al., 1998; Ali and Thomson, 1998). Our results demonstrate that the cell body of even this most narrowly defined cell type can be located in several layers; therefore, interneurons should not be pooled as functionally distinct populations on the basis of the laminar location of their cell bodies. The four axo-axonic cells differed from other cells of this type reported to date in their horizontal dendritic arborization. However, horizontal dendrites alone do not identify a cell type, as this characteristic is shared by such widely differing cells as O-LM and axo-axonic cells. Both the dendritic and axonal patterns of an individual cell need to be analyzed for identification and the interpretation of their place in the network. Based on our data, it is not possible to establish whether horizontal axo-axonic cells receive afferent inputs selectively from local pyramidal cells, or whether they gather similar inputs as axo-axonic cells with radial dendrites. Until direct tests on the consistency of synaptic inputs can be conducted, a parsimonious viewpoint is to keep all axo-axonic cells as one class of cell based on their synaptic output.

### Acknowledgments

The authors thank Dr. M. Capogna for helpful comments on an earlier version of this manuscript, Mr. J. David B. Roberts for help with electron microscopic analysis, and Mr. Philip Cobden, Mr. Paul Jays, and Ms. Neidja Gould for their technical assistance.

## REFERENCES


Aika Y, Ren JQ, Kosaka K, Kosaka T. 1994. Quantitative analysis of GABA-like-immunoreactive and parvalbumin-containing neurons in the CA1 region of the rat hippocampus using a stereological method, the dissector. Exp Brain Res 99:267–276.

Ali AB, Thomson AM. 1998. Facilitating pyramid to horizontal oriens-alveus interneurone inputs: dual intracellular recordings in slices of rat hippocampus. J Physiol 507:185–199.

Ali AB, Deuchars J, Pawelzik H, Thomson AM. 1998. CA1 pyramidal to basket and bistratified cell EPSPs: dual intracellular recordings in rat hippocampal slices. J Physiol 507:201–217.

Blasco-Ibanez JM, Freund TF. 1995. Synaptic input of horizontal interneurons in stratum oriens of the hippocampal CA1 subfield: structural basis of feed-back activation. Eur J Neurosci 7:2170–2180.

Buhl EH, Han ZS, Lorinczi Z, Stezhka VV, Karnup SV, Somogyi P. 1994. Physiological properties of anatomically identified axo-axonic cells in the rat hippocampus. J Neurophysiol 71:1289–1307.

Cauli B, Porter JT, Tsuzuki K, Lambolez B, Rossier J, Quenet B, Audinat E. 2000. Classification of fusiform neocortical interneurons based on unsupervised clustering. Proc Natl Acad Sci USA 97:6144–6149.

Chitwood RA, Jaffe DB. 1998. Calcium-dependent spike-frequency accommodation in hippocampal CA3 nonpyramidal neurons. J Neurophysiol 80:983–988.

Cobb SR, Halasy K, Vida I, Nyiri G, Tamas G, Buhl EH, Somogyi P. 1997. Synaptic effects of identified interneurons innervating both interneurons and pyramidal cells in the rat hippocampus. Neuroscience 79:629–648.

Cope DW, Maccaferri G, Marton LF, Roberts JD, Cobden PM, Somogyi P. 2002. Cholecystokinin-immunopositive basket and Schaffer collateral-associated interneurones target different domains of pyramidal cells in the CA1 area of the rat hippocampus. Neuroscience 109:63–80.

Deller T, Adelmann G, Nitsch R, Frotscher M. 1996. The alvear pathway of the rat hippocampus. Cell Tissue Res 286:293–303.

Feldmeyer D, Egger V, Lubke J, Sakmann B. 1999. Reliable synaptic connections between pairs of excitatory layer 4 neurones within a single "barrel" of developing rat somatosensory cortex. J Physiol 521: 169–190.

Freund TF, Antal M. 1988. GABA-containing neurons in the septum control inhibitory interneurons in the hippocampus. Nature 336:170–173.

Freund TF. 1992. GABAergic septal and serotonergic median raphe afferents preferentially innervate inhibitory interneurons in the hippocampus and dentate gyrus. Epilepsy Res 7(suppl):79–91.

Freund TF, Buzsaki G. 1996. Interneurons of the hippocampus. Hippocampus 6:347–470.

Freund TF, Gulyas AI, Acsady L, Gorcs T, Toth K. 1990. Serotonergic control of the hippocampus via local inhibitory interneurons. Proc Natl Acad Sci USA 87:8501–8505.

Fukuda T, Kosaka T. 2000. Gap junctions linking the dendritic network of GABAergic interneurons in the hippocampus. J Neurosci 20:1519–1528.

Fukuda T, Aika Y, Heizmann CW, Kosaka T. 1996. Dense GABAergic input on somata of parvalbumin-immunoreactive GABAergic neurons in the hippocampus of the mouse. Neurosci Res 26:181–194.

Gulyas AI, Gorcs TJ, Freund TF. 1990. Innervation of different peptide-containing neurons in the hippocampus by GABAergic septal afferents. Neuroscience 37:31–44.

Gulyas AI, Miles R, Sik A, Toth K, Tamamaki N, Freund TF. 1993. Hippocampal pyramidal cells excite inhibitory neurons through a single release site. Nature 366:683–687.

Gupta A, Wang Y, Markram H. 2000. Organizing principles for a diversity of GABAergic interneurons and synapses in the neocortex. Science 287:273–278.

Han ZS, Buhl EH, Lorinczi Z, Somogyi P. 1993. A high degree of spatial selectivity in the axonal and dendritic domains of physiologically identified local-circuit neurons in the dentate gyrus of the rat hippocampus. Eur J Neurosci 5:395–410.

Ishizuka N, Weber J, Amaral DG. 1990. Organization of intrahippocampal projections originating from CA3 pyramidal cells in the rat. J Comp Neurol 295:580–623.

Katona I, Acsady L, Freund TF. 1999. Postsynaptic targets of somatostatin-immunoreactive interneurons in the rat hippocampus. Neuroscience 88:37–55.

Katsumaru H, Kosaka T, Heizmann CW, Hama K. 1988. Immunocytochemical study of GABAergic neurons containing the calcium-binding protein parvalbumin in the rat hippocampus. Exp Brain Res 72:347–362.

Kawaguchi Y. 1995. Physiological subgroups of nonpyramidal cells with specific morphological characteristics in layer II/III of rat frontal cortex. J Neurosci 15:2638–2655.

Kawaguchi Y, Kubota Y. 1997. GABAergic cell subtypes and their synaptic connections in rat frontal cortex. Cereb Cortex 7:476–486.

Kawaguchi Y, Katsumaru H, Kosaka T, Heizmann CW, Hama K. 1987. Fast spiking cells in rat hippocampus (CA1 region) contain the calcium-binding protein parvalbumin. Brain Res 416:369–374.

Kölliker A. 1896. Handbuch der Gewebelehre des Menschen. Leipzig: Engelmann.

Kosaka T, Katsumaru H, Hama K, Wu JY, Heizmann CW. 1987. GABAergic neurons containing the $Ca^{2+}$-binding protein parvalbumin in the rat hippocampus and dentate gyrus. Brain Res 419:119–130.

Lacaille JC, Schwartzkroin PA. 1988. Stratum lacunosum-moleculare interneurons of hippocampal CA1 region. I. Intracellular response characteristics, synaptic responses, and morphology. J Neurosci 8:1400–1410.

Lacaille JC, Williams S. 1990. Membrane properties of interneurons in stratum oriens-alveus of the CA1 region of rat hippocampus in vitro. Neuroscience 36:349–359.

Lacaille JC, Mueller AL, Kunkel DD, Schwartzkroin PA. 1987. Local circuit interactions between oriens/alveus interneurons and CA1 pyramidal cells in hippocampal slices: electrophysiology and morphology. J Neurosci 7:1979–1993.

Li XG, Somogyi P, Tepper JM, Buzsaki G. 1992. Axonal and dendritic arborization of an intracellularly labeled chandelier cell in the CA1 region of rat hippocampus. Exp Brain Res 90:519–525.

Li XG, Somogyi P, Ylinen A, Buzsaki G. 1994. The hippocampal CA3 network: an in vivo intracellular labeling study. J Comp Neurol 339: 181–208.

Lorente de Nó R. 1934. Studies on the structure of the cerebral cortex. II. Continuation of the study of the ammonic system. J Psychol Neurol 46:113–177.

Maccaferri G, McBain CJ. 1995. Passive propagation of LTD to stratum oriens-alveus inhibitory neurons modulates the temporoammonic input to the hippocampal CA1 region. Neuron 15:137–145.

Maccaferri G, Roberts JD, Szucs P, Cottingham CA, Somogyi P. 2000. Cell surface domain specific postsynaptic currents evoked by identified GABAergic neurones in rat hippocampus in vitro. J Physiol 524:91–116.

McBain CJ, DiChiara TJ, Kauer JA. 1994. Activation of metabotropic glutamate receptors differentially affects two classes of hippocampal interneurons and potentiates excitatory synaptic transmission. J Neurosci 14:4433–4445.

Morin F, Beaulieu C, Lacaille JC. 1996. Membrane properties and synaptic currents evoked in CA1 interneuron subtypes in rat hippocampal slices. J Neurophysiol 76:1–16.

Mott DD, Turner DA, Okazaki MM, Lewis DV. 1997. Interneurons of the dentate-hilus border of the rat dentate gyrus: morphological and electrophysiological heterogeneity. J Neurosci 17:3990–4005.

Oliva AA Jr, Jiang M, Lam T, Smith KL, Swann JW. 2000. Novel hippocampal interneuronal subtypes identified using transgenic mice that

express green fluorescent protein in GABAergic interneurons. J Neurosci 20:3354–3368.
Parra P, Gulyas AI, Miles R. 1998. How many subtypes of inhibitory cells in the hippocampus? Neuron 20:983–993.
Pawelzik H, Hughes DI, Thomson AM. 2002. Physiological and morphological diversity of immunocytochemically defined parvalbumin- and cholecystokinin-positive interneurones in CA1 of the adult rat hippocampus. J Comp Neurol 443:346–367.
Pedarzani P, Kulik A, Muller M, Ballanyi K, Stocker M. 2000. Molecular determinants of $Ca^{2+}$-dependent $K^{+}$ channel function in rat dorsal vagal neurones. J Physiol 527:283–290.
Peters A, Palay SL, Webster H deF. 1991. The fine structure of the nervous system. Neurons and their supporting cells. 3rd ed. New York: Oxford University Press.
Pike FG, Goddard RS, Suckling JM, Ganter P, Kasthuri N, Paulsen O. 2000. Distinct frequency preferences of different types of rat hippocampal neurones in response to oscillatory input currents. J Physiol 529:205–213.
Pikkarainen M, Ronkko S, Savander V, Insausti R, Pitkanen A. 1999. Projections from the lateral, basal, and accessory basal nuclei of the amygdala to the hippocampal formation in rat. J Comp Neurol 403: 229–260.
Ramon y Cajal S. 1893. Estructura del asta de ammon y fascia dentata. Anal Soc Espan Hist Nat 22:53–114.
Sakmann B, Stuart G. 1995. Patch-pipette recordings from the soma, dendrites and axon of neurones in brain slices. In: Sakmann B, Neher E, editors. Single-channel recording. New York: Plenum Press. p 199–211.
Sala L. 1891. Zur feineren Anatomie des grossen Seepferdefusses. Z Wissenschaft Zool 52:18–45.
Savic N, Pedarzani P, Sciancalepore M. 2001. Medium afterhyperpolarization and firing pattern modulation in interneurons of stratum radiatum in the CA3 hippocampal region. J Neurophysiol 85:1986–1997.
Schwartzkroin PA, Kunkel DD. 1985. Morphology of identified interneurons in the CA1 regions of guinea pig hippocampus. J Comp Neurol 232:205–218.
Sik A, Penttonen M, Ylinen A, Buzsaki G. 1995. Hippocampal CA1 interneurons: an in vivo intracellular labeling study. J Neurosci 15: 6651–6665.
Somogyi P. 1977. A specific "axo-axonal" interneuron in the visual cortex of the rat. Brain Res 136:345–350.
Somogyi P, Nunzi MG, Gorio A, Smith AD. 1983. A new type of specific interneuron in the monkey hippocampus forming synapses exclusively with the axon initial segments of pyramidal cells. Brain Res 259:137–142.
Somogyi P, Freund TF, Hodgson AJ, Somogyi J, Beroukas D, Chubb IW. 1985. Identified axo-axonic cells are immunoreactive for GABA in the hippocampus and visual cortex of the cat. Brain Res 332:143–149.
Somogyi P, Tamas G, Lujan R, Buhl EH. 1998. Salient features of synaptic organisation in the cerebral cortex. Brain Res Brain Res Rev 26:113–135.
Stuart GJ, Dodt HU, Sakmann B. 1993. Patch-clamp recordings from the soma and dendrites of neurons in brain slices using infrared video microscopy. Pfluegers Arch 423:511–518.
Waldeck RF, Pereda A, Faber DS. 2000. Properties and plasticity of paired-pulse depression at a central synapse. J Neurosci 20:5312–5320.
Woodson W, Nitecka L, Ben-Ari Y. 1989. Organization of the GABAergic system in the rat hippocampal formation: a quantitative immunocytochemical study. J Comp Neurol 280:254–271.
Zhang L, McBain CJ. 1995a. Potassium conductances underlying repolarization and after-hyperpolarization in rat CA1 hippocampal interneurones. J Physiol 488:661–672.
Zhang L, McBain CJ. 1995b. Voltage-gated potassium currents in stratum oriens-alveus inhibitory neurones of the rat CA1 hippocampus. J Physiol 488:647–660.